On the Existence of Storm-Tracks

BRIAN J. HOSKINS AND PAUL J. VALDES

Department of Meteorology, University of Reading, Reading, United Kingdom

(Manuscript received 5 June 1989, in final form 15 January 1990)

ABSTRACT

Given that middle latitude weather systems transport heat in a manner such as to weaken the baroclinicity that is thought to be crucial to their growth, it is perhaps surprising that concentrated regions of such eddy activity, i.e. storm-tracks, are found in the Northern Hemisphere winter. The existence and possible self-maintenance of storm-tracks is investigated using a linear, stationary wave model with storm-track region forcings taken from data averaged over a number of winters. It is found that the direct thermal effect of the eddies does indeed act against the existence of the storm-track. Their vorticity fluxes lead to some reduction of this effect. It is argued that the mean diabatic heating in the storm-track region is an indirect eddy effect. This heating is found to maintain the mean maximum in baroclinicity in the region. Further, the mean low-level flow induced by the eddy effects is such as to enhance the warm western oceanic boundary currents that are crucial to the existence of the storm-tracks. The extent to which the Northern Hemisphere storm-tracks can be considered self-maintaining is discussed.

1. Introduction

The diagnostic work of Blackmon (1976) and Lau and Wallace (1979) has demonstrated the existence in Northern Hemisphere winter data of latitudinally confined regions of large 2–6 day height-field variance extending from the east coasts of North America and Asia across the Atlantic and Pacific oceans, respectively. As discussed recently by Wallace et al. (1988) these regions are not quite the traditional storm-tracks defined by following low pressure centers—the latter being biased towards regions of mean low pressure. However, in this paper this name will be used for them.

Figure 1 shows a summary of some of the features of the Northern Hemisphere storm-tracks as defined by six winters of data from the European Centre for Medium Range Weather Forecasts (ECMWF). Upstream of the two regions of maximum synoptic time scale height-field variance ($\overline{\phi'^2}$) are maxima of poleward ($\overline{v'T'}$) and upward ($-\overline{\omega'T'}$) heat flux by these systems. The arrows in Fig. 1 indicate $\mathbf{E} = (\overline{v'^2}-\overline{u'^2}, -\overline{u'v'})$ at 250 mb. As shown by Hoskins et al. (1983), where these arrows diverge there is a tendency to force the mean westerly flow. Also indicated in Fig. 1 are the regions, poleward of 20°N, of maximum column-averaged diabatic heating. This field is computed as a residual in the thermodynamic equation. The heating regions start off the east coasts, to the south of the storm-track. Here it is quite shallow and is presumably associated with significant sensible heating at the surface, with shallow convection redistributing it in the vertical up to 850 mb. The diabatic heating maxima extend westward and slightly poleward into the storm-tracks where they are deeper and probably dominated by latent heat release. The sensible heating will occur predominantly in the flow of cold air off the continents over warm waters that occurs behind mobile low pressure systems, and the latent heat release will be mostly in the warm moist air that is rising ahead of them. Radiative effects due to increased cloud cover may also play a role (Stephens and Webster 1979). Consequently the diabatic heating maxima owe much of their existence to the presence of the storm-tracks. This relationship between storm-tracks and thermal forcing was first discussed by Sutcliffe (1951).

Midlatitude weather systems are believed to have their origin in processes encapsulated in the theory of baroclinic instability. A suitable measure of the baroclinicity is provided by the Eady growth rate maximum:

$$\sigma_{BI} = 0.31 f |\partial \mathbf{v}/\partial z| N^{-1},$$

(the notation being standard). Lindzen and Farrell (1980) have shown that this formula provides an accurate estimate of the growth rate maximum in a range of baroclinic instability problems, although James (1987) has cautioned that low-level horizontal shears can reduce the attainable value. Moist processes generally lead to an increase in growth rate (e.g., Emanuel et al. 1987) and it might be thought appropriate to use some reduced effective static stability in σ_{BI}. However, such complexity will be neglected here.

Life-cycle experiments (e.g., Simmons and Hoskins

Corresponding author address: Dr. Brian J. Hoskins, Department of Meteorology, University of Reading, 2 Earley Gate, Whiteknights, Reading RG6 2AU, United Kingdom.

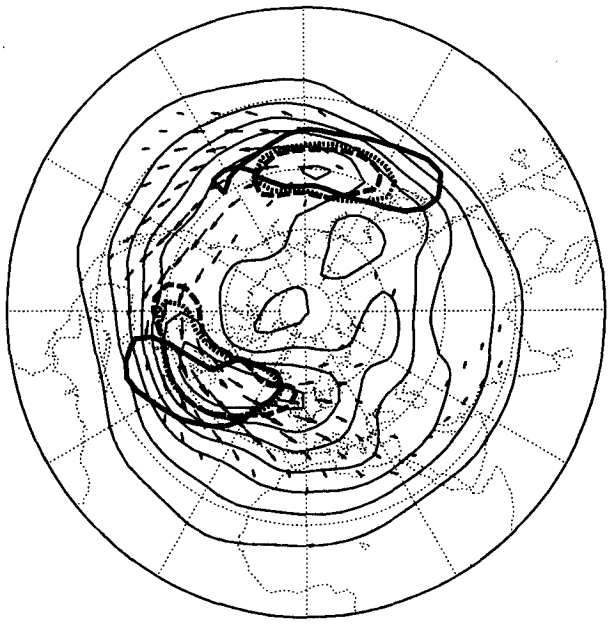

FIG. 1. A summary of the Northern Hemisphere winter storm-track structure based on high-pass time-filtered transients in ECMWF data for the December–February season in the years 1979–84. The thin contours are of height variance $(\overline{\phi'^2})$ (contour interval 15 m^2) and arrows indicate E = $(\overline{v'^2}-\overline{u'^2}, -\overline{u'v'})$, both at 250 mb. Also shown are single contours of the 700 mb horizontal temperature flux $(\overline{v'T'})$ (thick dashed contour at 10 K m s^{-1}), 700 mb vertical temperature flux $(-\overline{\omega'T'})$ (thick dotted contour at 0.2 K Pa s^{-1}), and the column mean diabatic heating (thick solid contour at 50 W m^{-2}).

1980) have suggested that the baroclinicity through some depth of the troposphere is important in the amplitudes achieved by nonlinear modes. Very close to the surface, variations in N, in particular, would tend to dominate but these are not relevant in nonlinear baroclinic instability. Consequently we shall determine σ_{BI} by using finite differences over a depth of about 2 km just above the boundary layer. At these levels, the longitudinal variations of σ_{BI} are dominated by the shear term. Changes in N are only important at high latitudes, particularly near Greenland.

Figure 2 shows σ_{BI} in units of day^{-1} for a Northern Hemisphere winter mean. The two regions in which the storm-track heat fluxes are found are picked out remarkably well by this measure of the baroclinicity. The Atlantic and Pacific maxima correspond to amplifications by factors of about 2 and 3 in a day, respectively, whereas elsewhere at similar latitudes the factor is nearer 1.5. At the ends of both storm-tracks are minima in σ_{BI}. An alternative measure of the baroclinicity is the parameter

$$r = f^2|\partial \mathbf{v}/\partial z|(\beta N^2 H_s)^{-1}$$

which was introduced by Charney (1947) and used by Held (1978) in the form $r = h/H_s$, where H_s is the density scale height. The height scale of the mode is h, provided that this is less than H_s, i.e. $r \leqslant 1$. For $r \geqslant 1$, the height scale is H_s. Since $r \propto \sigma_{BI} N^{-1} \tan\phi$, a plot of r exhibits similar information except that polar regions are given extra prominence. Numerically,

$$r \approx 2.7\tilde{\sigma}_{BI} \tan\phi \tilde{N}^{-1}$$

where $\tilde{\sigma}_{BI}$ is σ_{BI} measured in units of day^{-1}, as in Fig. 2, and $\tilde{N}$ is N measured in units of $(1.1\ 10^2\ s)^{-1}$. Thus Fig. 2 suggests deep baroclinic instability over the storm-track regions. However, over North Africa and the Middle East the local maximum in growth rate would correspond only to shallow systems. The deductions from Fig. 2 are in agreement with the linear baroclinic instability calculations for a longitudinally varying Northern Hemisphere winter flow exhibited by Frederiksen (1983).

Thus the time-mean flow is consistent with the existence of the storm-track but one may question whether the reverse is true. If a midlatitude weather system grows in a region of high baroclinicity, by transporting heat poleward it acts to reduce this baroclinicity. For example, in the downstream development calculations of Simmons and Hoskins (1979), the packet of baroclinic wave activity leaves behind a region of negligible low-level and midlatitude baroclinicity, the potential temperature contours being pushed far to the north and south. Thus one would not expect the next systems to follow the same track but rather to move at a different latitude or develop in a different region. However, this runs counter both to synoptic

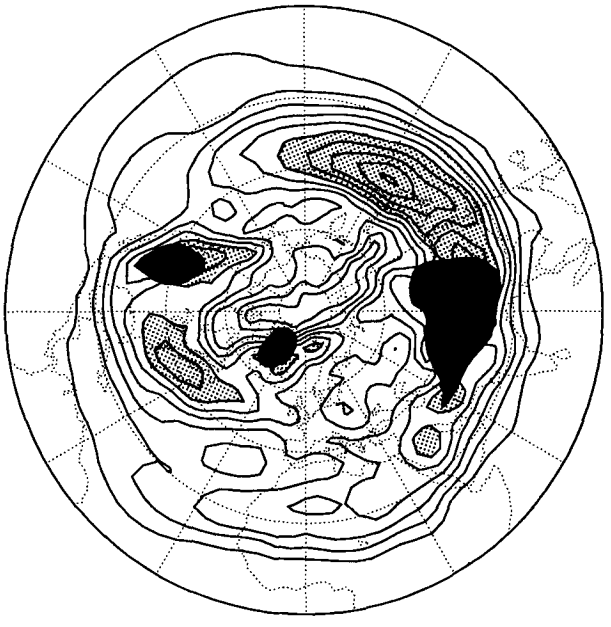

FIG. 2. The baroclinicity parameter $\sigma_{BI} = 0.31\ f|\partial \mathbf{v}/\partial z|N^{-1}$ at about 780 mb for the Northern Hemisphere winter mean. The contours are drawn every 0.1 day^{-1} with zero at the equator and values below 0.1 day^{-1} at the North Pole. The stippling indicates values in excess of 0.6 day^{-1}. The region in which the 780 mb level is within 1 km of the orography and, therefore, probably in the boundary layer, is blacked.

experience and to the notion of storm-tracks discussed above.

The nature of the vorticity fluxes by the high-pass transients was investigated by Hoskins et al. (1983). The divergence of the *E*-vectors in the storm-tracks shown in Fig. 1 indicates a tendency to produce cyclonic circulation on the poleward side and anticyclonic circulation on the equatorward flank. In a longitudinally confined storm-track this implies a tendency to create confluence at the upstream end. If this is sufficiently strong it could act to maintain the mean baroclinicity against the destructive tendency of the heat transports.

In this paper this problem is investigated using a baroclinic model that is linearized about the observed December–February time-averaged zonal flow and for which steady solutions can be obtained for any prescribed forcing. This model and its solutions for climatological forcing terms have recently been described in some detail by Valdes and Hoskins (1989). When forcing by diabatic heating, orography, and transient flux divergences are included, the wave solution is generally close to that observed. This suggests that it can be used in the present context for discussing the response to particular forcings.

A very brief description of the model and data are given in section 2. Section 3 presents the results for forcings associated with the Atlantic storm-track. In particular, the baroclinicity for particular solutions, as measured by σ_{BI}, is displayed. A brief comparison of the Pacific storm-track is given in section 4 and some concluding remarks are made in section 5.

2. The model and data

The model is based on the σ-coordinate spectral model described by Hoskins and Simmons (1975). It is linearized about a zonal flow and for any prescribed forcing the stationary response can be determined by solving a set of linear equations. As in Valdes and Hoskins (1989), the model used here has 15 levels and a triangular truncation at total wavenumber 31. The damping terms take the form of a Rayleigh drag and Newtonian cooling plus a hyperdiffusion. The lowest two levels $\sigma = 0.89$ and $\sigma = 0.96$ have drag time scales of 2.5 and 0.5 days, respectively, and cooling time scales of 12 and 5.5 days, respectively. In the free atmosphere there is no drag and the cooling time-scale is 25 days. The top three levels, above $\sigma = 0.1$, have enhanced damping to inhibit spurious reflections.

Data for calculations came from a 6-year (1979–84) climatology of ECMWF December–February (DJF) initialized analysis. Variables are available on twelve pressure levels. Synoptic time scale transients are produced by the time filter described in Lau et al. (1981), which is based on the "poor man's" spectral analysis of Lorenz (1979). Its effect is similar to the 2.5–6 day bandpass filter used by Blackmon (1976). Net diabatic heating is deduced as a residual in the thermodynamic equation. As discussed in Valdes and Hoskins (1989) the resulting field is quite credible except that for the early years of ECMWF data the divergent flow in the tropics was underestimated and the computed diabatic heating is consequently too weak there. All fields have been spatially smoothed using the technique described in Sardeshmukh and Hoskins (1984), with $a = 0.1$ and $n = 24$.

3. The Atlantic storm-track

In this section only mean forcing terms associated with the 20°–80°N, 80°W–20°E region will be considered. In order to illustrate some aspects of this forcing, longitudinal averages across the sector are shown in Fig. 3. Note that because of the slight SW–NE tilt of the Atlantic storm-track, such zonal averaging produces some smoothing. The convergence of the high-pass horizontal temperature flux (Fig. 3a) shows deep heating near 55°N and cooling near 35°N of about 0.5 K day^{-1}. The upward flux of potential temperature produces lower tropospheric cooling of more than 1 K day^{-1} and upper tropospheric warming (Fig. 3b). The sum of these thermal flux convergences (Fig. 3c) illustrates the "sloping convection" nature of midlatitude weather systems whereby they act to cool the atmosphere at low levels near 40°N and heat it at upper tropospheric levels near 55°N. With the rather crude filter used here, the magnitudes are near 1 K day^{-1}. The other fields in Fig. 3 will be discussed below.

The steady-state response to the total thermal forcing due to transient fluxes is summarized in Fig. 4. As in Valdes and Hoskins (1989) the streamfunction perturbations are shown at $\sigma = 0.20$ (level 5) and 0.89 (level 14), which will be referred to as the upper and lower level, respectively. The upper level flow (Fig. 4a) shows a high latitude cyclone and anticyclone, an elongated cyclone at 30°N and anticyclone at 15°N. Near 45°N the westerlies are enhanced over North America and decreased near western Europe. The low-level flow (Fig. 4b) shows a cyclone–anticyclone couplet with enhanced westerlies over the Atlantic near 45°N. Consistent with the forcing shown in Fig. 3c, the low-level thermal perturbation (Fig. 4c) is negative. If the perturbation solution is added to the basic zonal flow then the baroclinicity parameter distribution is that given in Fig. 4d. It exhibits a minimum in the Atlantic storm-track region as was anticipated in the discussion in the Introduction. Thus, the direct thermal effects of midlatitude weather systems act to oppose the existence of the storm-track. It is of interest to note that the vertical potential temperature flux term has an important impact on the low-level thermal perturbation but, because of the rich vertical structure of the forcing term its impact on the streamfunction is small. (In potential vorticity terms, the cooling at the surface is equivalent to a negative forcing, the increase of heat-

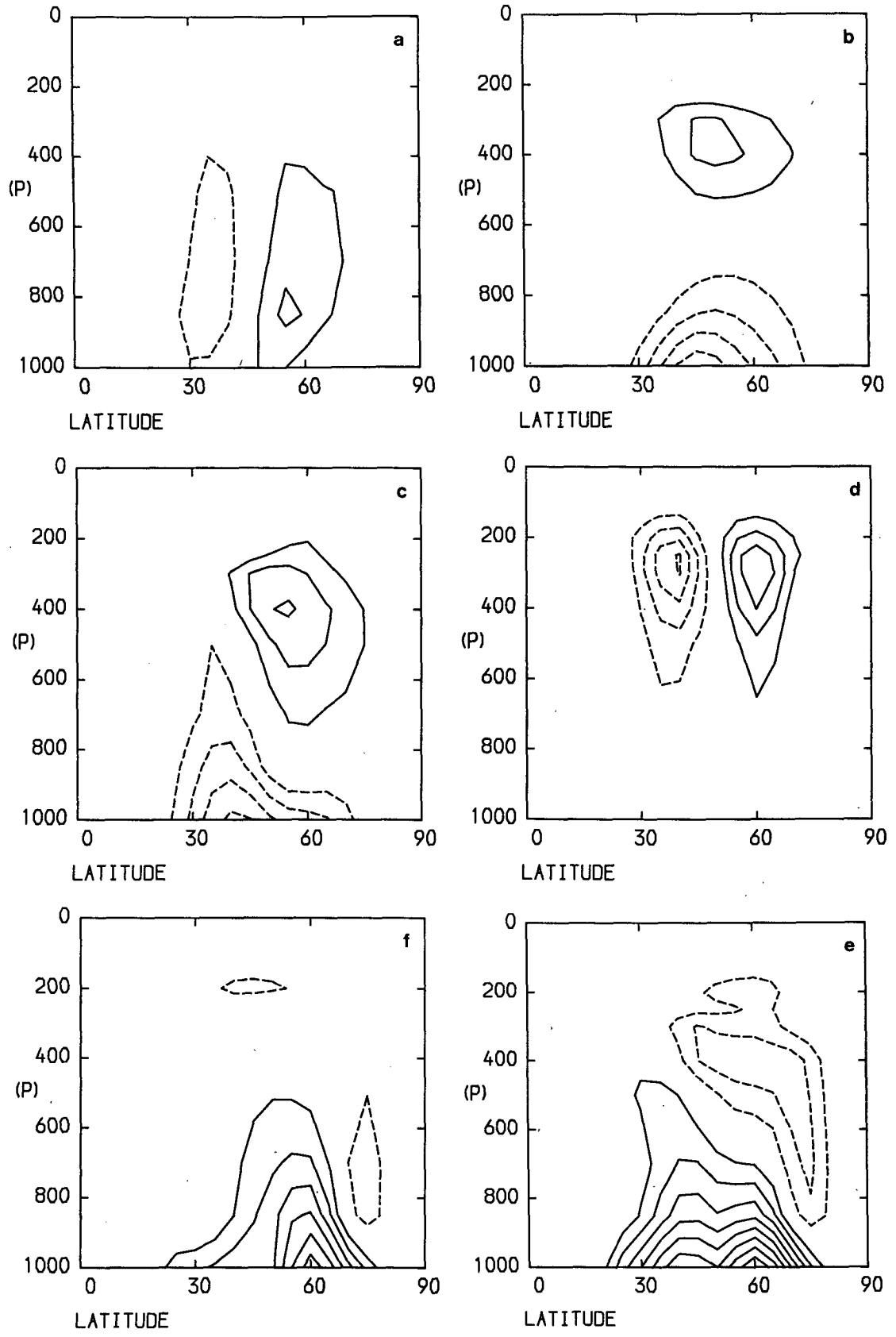

FIG. 3. Latitude–height structure of winter North Atlantic forcings zonally averaged from 80°W to 20°E. Shown are (a) the high pass horizontal temperature flux convergence, (b) the high pass vertical potential temperature flux convergence multiplied by $(p/p_0)^{\kappa}$, (c) the total direct thermal effect of the high-pass eddies (sum of a and b), (d) the high-pass horizontal vorticity flux convergence, (e) the mean diabatic heating, and (f) the total thermal forcing (sum of c and e). The contour unit in (d) is 4.0×10^{-12} s^{-2} and in the other plots it is 0.25 K day^{-1}. Negative contours are dashed and the zero contour is not drawn.

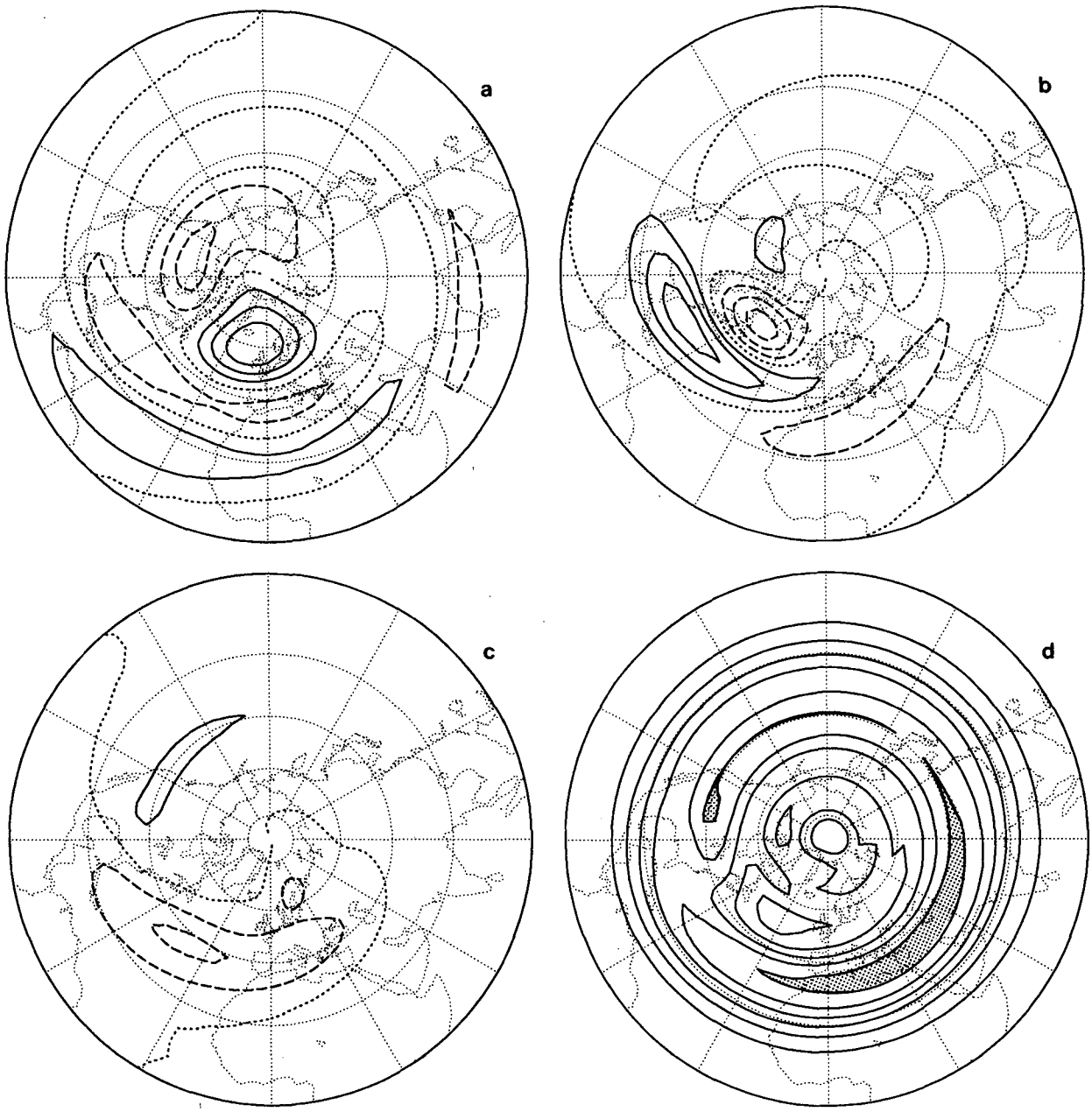

FIG. 4. The steady state linear response to North Atlantic direct thermal forcing by the synoptic time scale transients. Shown are (a) the streamfunction perturbation at the upper level, $\sigma = 0.20$; contour interval $5 \times 10^{-4}\ \Omega\ a^2$ (approximately $1.5 \times 10^6\ m^2\ s^{-1}$), (b) the streamfunction perturbation at the lower level, $\sigma = 0.89$; contour interval half that of (a), (c) the temperature perturbation at the lower level, $\sigma = 0.89$; contour interval 2 K, (d) the baroclinicity parameter σ_{BI} as in Fig. 2 for the zonal flow plus the perturbation.

ing with height in the troposphere gives a positive forcing, and the decrease with height near the tropopause implies a negative forcing.)

As discussed in Valdes and Hoskins (1989), the transient forcing in the mean divergence equation is negligible, and the vorticity flux-convergence is well approximated for our purposes by its horizontal part, determined using the approximation that the eddies are nondivergent. The North Atlantic sector zonal-average tendency in the vorticity equation due to the high-pass transients is given in Fig. 3d and illustrates the tendency to accelerate the westerlies near 50°N. The linear solution is illustrated in Fig. 5. The upper level streamfunction anomaly shows a downstream response to the forcing and some equatorward wave propagation. The lower level response (not shown) is similar in the

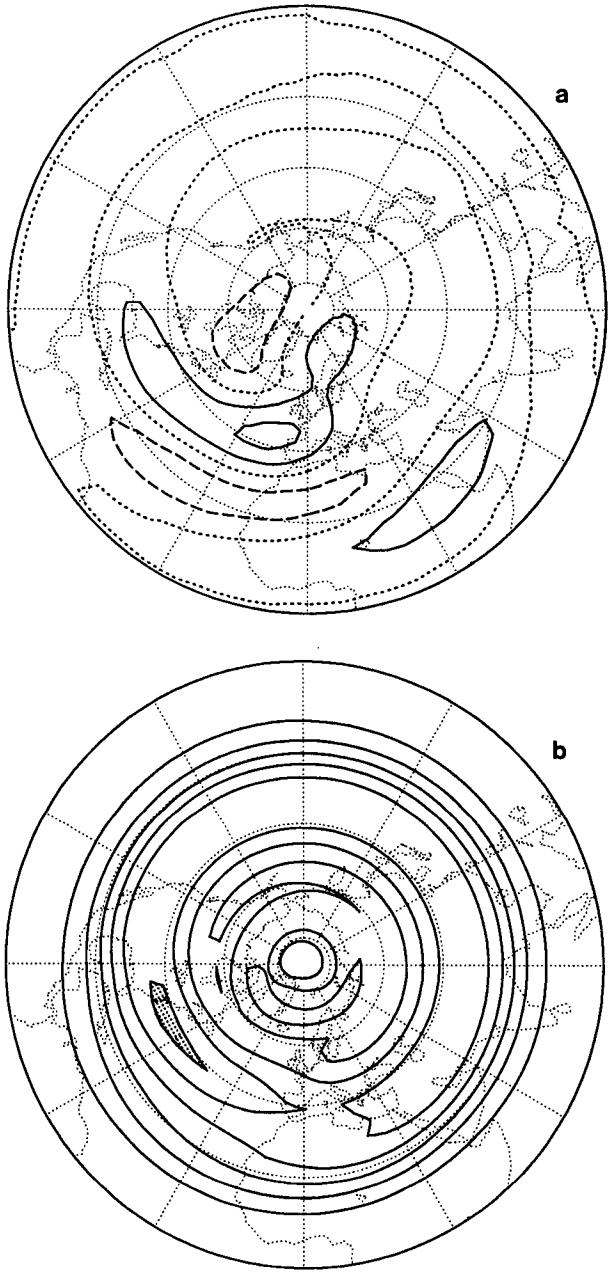

FIG. 5. The steady state, linear response to Northern Atlantic vorticity forcing by the synoptic time scale transients. Shown are (a) the upper level streamfunction and (b) the baroclinicity parameter σ_{BI}. The conventions are as in Fig. 4a, d.

North Atlantic but smaller in magnitude by a factor of 2–3. The lower level thermal response is not shown as it would have only the zero contour. However, the baroclinicity is shown in Fig. 5b. In agreement with Hoskins (1983), the vorticity flux by the high pass transients does lead to increased baroclinicity in the storm-track. However, the effect is weaker than the reduction caused by the thermal fluxes.

Valdes and Hoskins (1989) show that, when diabatic, orographic, and transient terms are used to force the stationary wave model used here, it simulates the mean planetary waves in the Northern Hemisphere with some accuracy. In particular, it produces the enhanced storm-track baroclinicity. If remote diabatic heating, orography, or low-frequency transients are crucial to this, the storm-tracks are not self-maintaining. On the contrary, their existence would be due to the inefficiency of the weather systems in weakening the storm-track baroclinicity. However, in the introduction it has been argued that the diabatic heating in the two storm-track regions can be considered to be predominantly due to the presence of the storm-tracks. Thus, we now consider the response to the diabatic heating in the North Atlantic sector. Figure 3e gives the sector zonal-average distribution of this heating. The low-level heating of almost 2.5 K day^{-1} is the result of local values of more than 7 K day^{-1} associated probably with sensible heating. The negative values are mainly a result of the sector including a substantial region of continental cooling and are therefore not directly related to the storm-track.

The response to this North Atlantic heating is shown in Fig. 6. The region from Florida to northwest Europe has a cyclonic anomaly at low-levels and an anticyclone at upper levels. At upper levels there is propagation into the equatorial region and also a high latitude response that is very sensitive to the zonal wind speeds in that region. At low levels there is an anticyclone poleward of the cyclone. If the diabatic forcing in a column is set to zero in regions in which the original column mean diabatic heating was negative, then this anticyclone disappears but other changes are small. The low-level temperature field shows positive values filling the North Atlantic and into northwest Europe. At the lowest model level ($\sigma = 0.97$) the values reach 12 K. The magnitude and vertical structure of the heating results in the linear solution (perturbation plus zonal mean) being statically unstable near the surface, especially in the vicinity of Greenland. A nonlinear steady-state model forced in this manner would have to include additional convective parameterization terms that would effectively change the forcing.

Finally, in Fig. 6d the baroclinicity parameter, σ_{BI}, is shown. The Atlantic storm-track maximum is now picked out beautifully. In fact, it is about 50% stronger than the climatological maximum shown in Fig. 2. The climatological maximum to the east of Greenland is also present but overemphasized. This is related to the excessively low static stability simulated by the linear model. Elsewhere the effect on σ_{BI} of variations in N are comparable or smaller then changes in $\mathbf{v}_z$.

The North Atlantic sector averaged, time-mean heating due to diabatic processes and high-pass transient fluxes is given in Fig. 3f. This total high-pass eddy heating is dominated by the diabatic term. The response to this and the vorticity flux, i.e. the sum of the

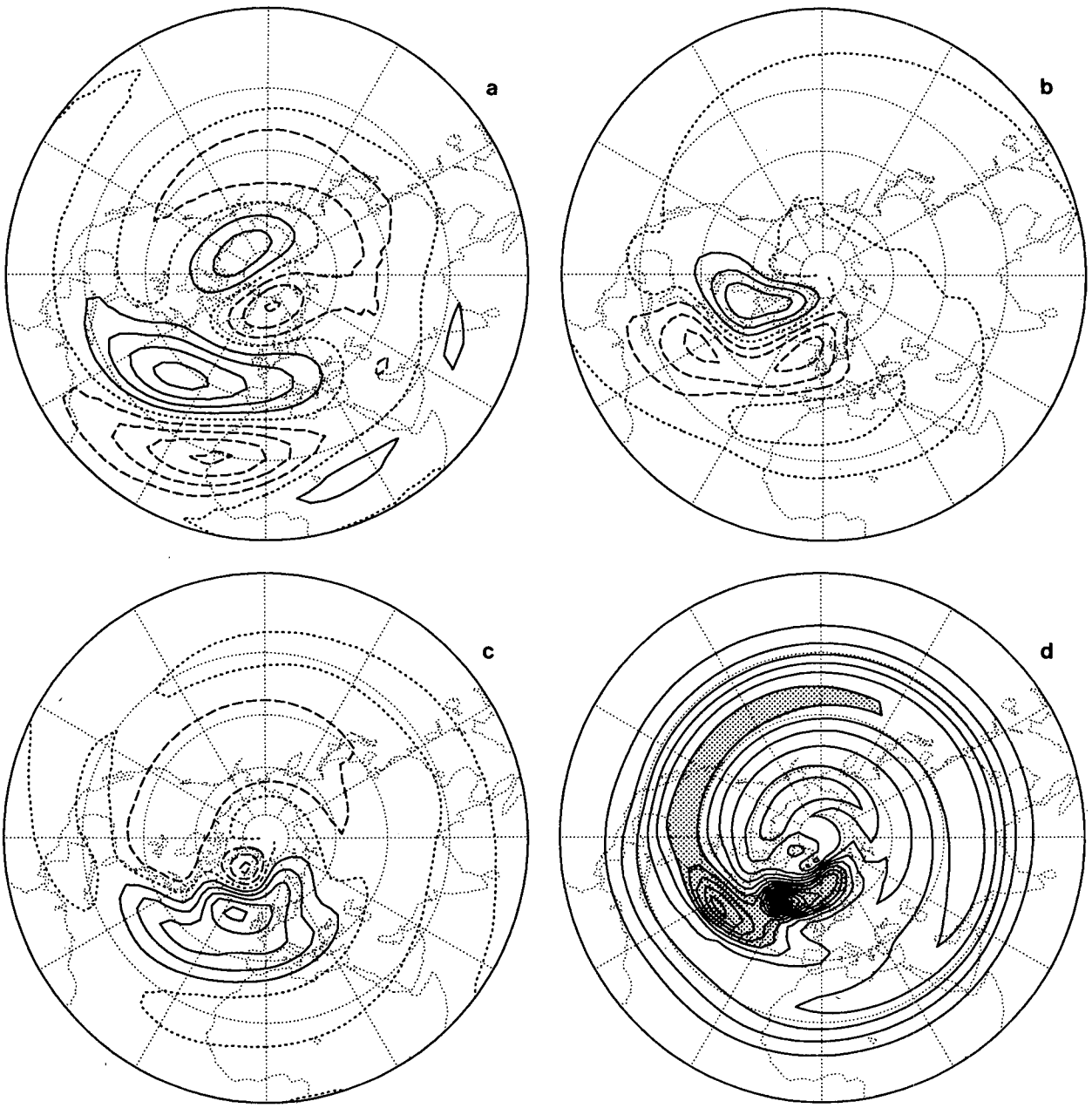

FIG. 6. The steady state, linear response to North Atlantic diabatic heating. Shown are (a) the upper level streamfunction, (b) the lower level streamfunction, (c) the lower level temperature, and (d) the baroclinicity parameter σ_{BI}. The conventions are as in Fig. 4.

results in Figs. 4, 5, and 6, is illustrated in Fig. 7. The upper level streamfunction is dominated by the part associated with the diabatic heating, but the strength of the anticyclone over northwest Europe is associated with the transient flux terms. The lower level streamfunction shows a large measure of cancellation between the transient eddy and diabatic heating forcings, leaving an Icelandic cyclonic anomaly associated mainly with the latter. The lower level temperature and σ_{BI} are dominated by the same component. The North Atlantic storm-track maximum in σ_{BI} is now reduced by the heat flux component to a value comparable to that observed. (Note that since σ_{BI} is a nonlinear diagnostic, Fig. 7d is not just the sum of the previous results.) In northwest Europe there is a minimum in σ_{BI} similar to that in Fig. 2 that provides a definite end to the storm-track.

The inclusion of the forcing due to remote diabatic heating, orography, low-frequency transients, and remote high-frequency transients modify the stationary wave solution and the associated σ_{BI}. However, the distribution of the latter is still dominated by the pattern

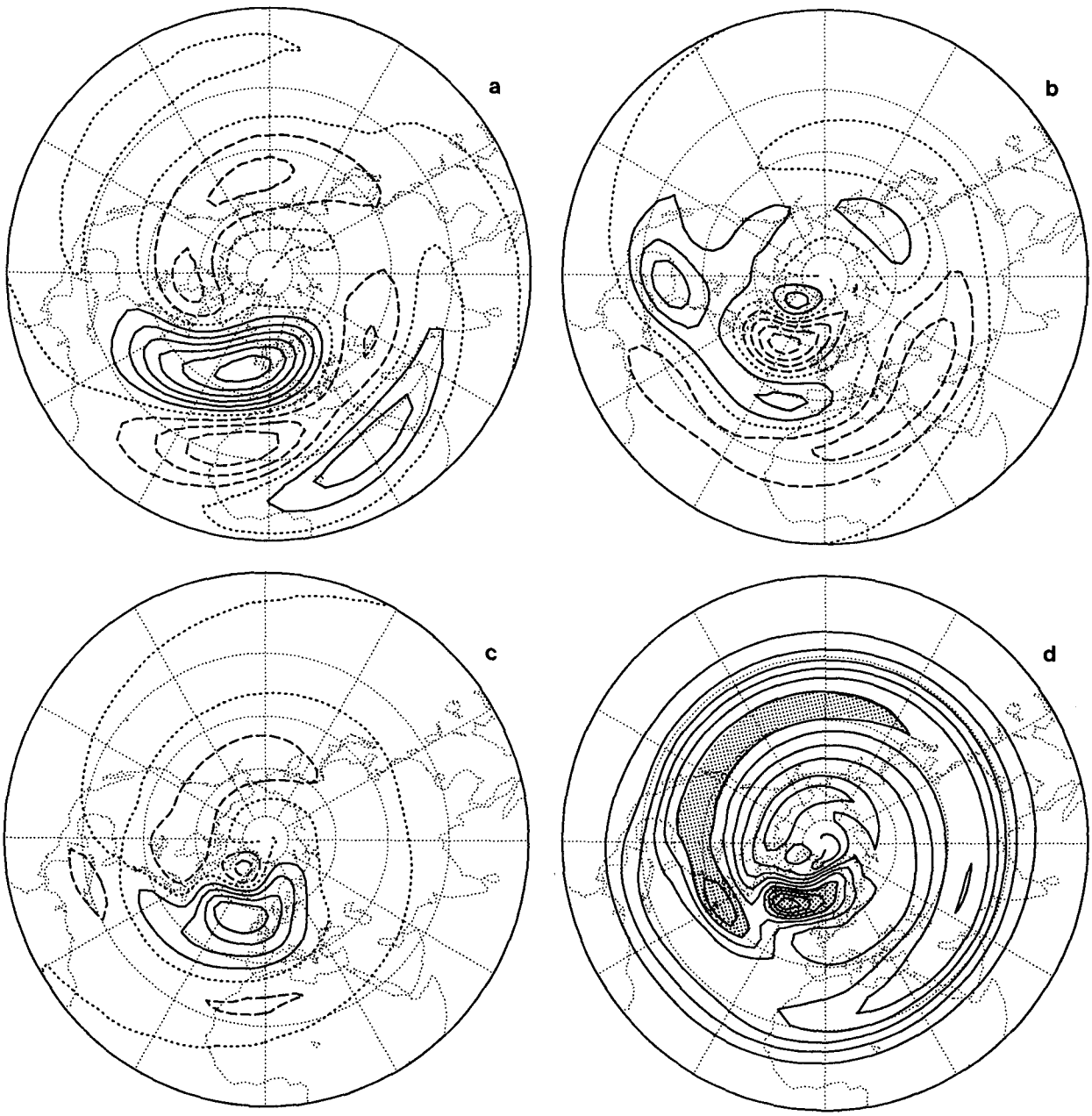

FIG. 7. The steady state, linear response to North Atlantic forcing by synoptic time scale transients and mean diabatic heating. Shown are (a) the upper level streamfunction, (b) the lower level streamfunction, (c) the lower level temperature, and (d) the baroclinicity parameter σ_{BI}. The conventions are as in Fig. 4.

imposed by the diabatic heating local to the storm-track regions. Remote responses tend to be of an equivalent barotropic nature with only small potential temperature perturbations.

4. The Pacific storm-track

In order to encompass all the relevant transient activity the sector is now defined as 110°E eastward to 100°W and 20°–80°N. The sector zonal-average forcings are similar to those shown in Fig. 3 but are generally displaced some 5°–10° equatorward, and are sharper because the storm-track itself is much more zonally oriented.

The responses to the various Pacific forcings are generally similar to the corresponding ones for the Atlantic. As a summary of these solutions we present the baroclinicity parameter for the separate cases (Fig. 8) and aspects of the total solution (Fig. 9). σ_{BI} for the direct thermal effect of the eddies (Fig. 8a) again ex-

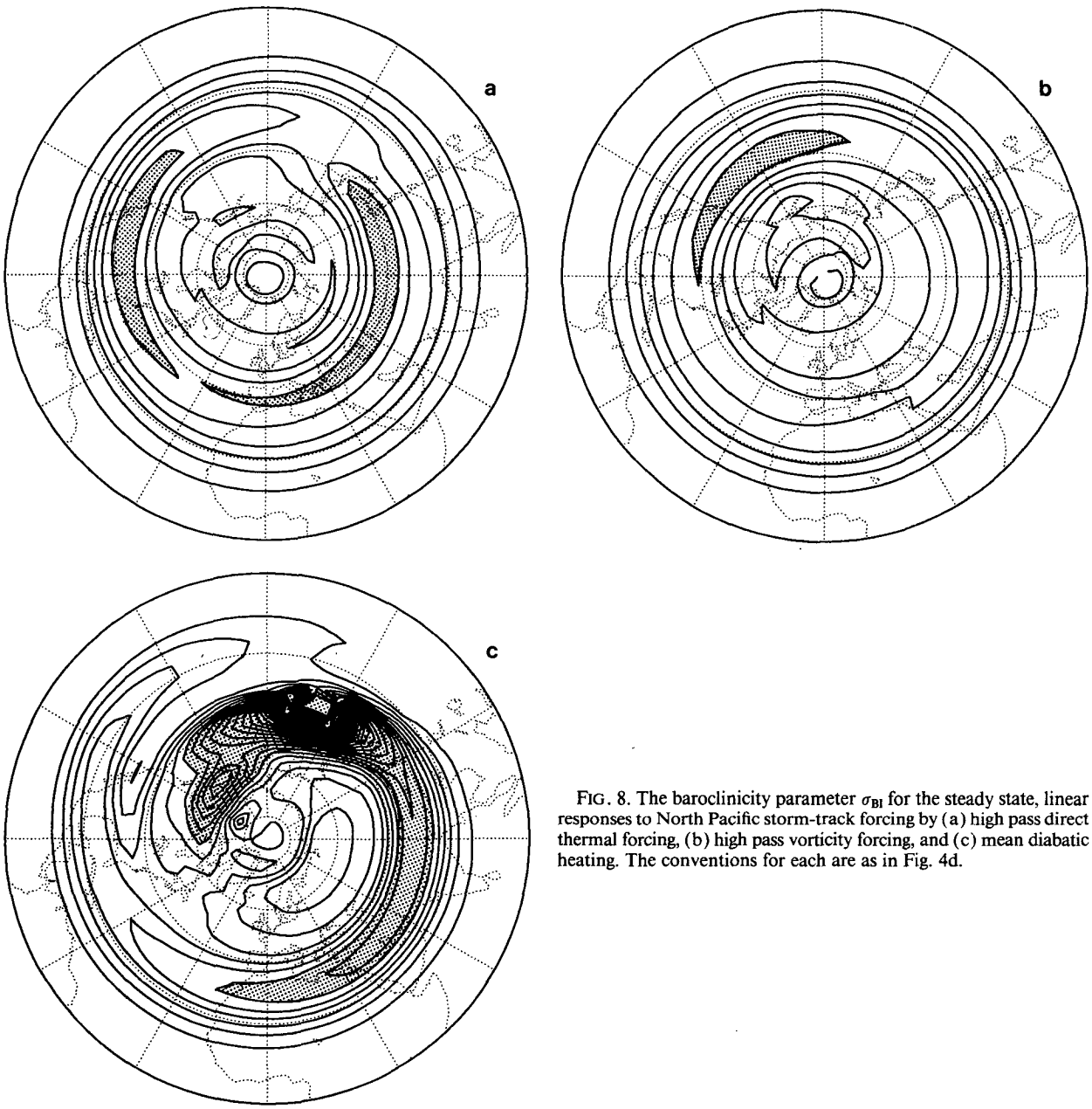

FIG. 8. The baroclinicity parameter σ_{BI} for the steady state, linear responses to North Pacific storm-track forcing by (a) high pass direct thermal forcing, (b) high pass vorticity forcing, and (c) mean diabatic heating. The conventions for each are as in Fig. 4d.

hibits a minimum in the actual growth region. The vorticity flux convergence solution (Fig. 8b) has a very weak maximum downstream of that observed and the diabatic heating σ_{BI} (Fig. 8c) exhibits a storm-track σ_{BI} maximum stronger than that observed.

The upper level response in the total solution (Fig. 9a) is qualitatively similar to that for the Atlantic (Fig. 7a), and is even more dominated by the diabatic heating portion. The lower level streamfunction anomaly (Fig. 9b) has less cancellation between the indirect and direct thermal forcing solutions than in the Atlantic case and the resulting Aleutian cyclonic anomaly is much more extended than its Icelandic counterpart. The indirect, diabatic component dominates but the direct transient thermal-flux response contributes positively in the east Pacific. The lower level positive temperature anomaly off the east coast of Asia, associated with diabatic heating, remains in the full solution (Fig. 9c) because the weaker negative anomalies associated with the direct thermal forcing are further downstream. The baroclinicity parameter (Fig. 9d) again picks out well the observed storm-track maximum, though the maximum value is too large in this case. However, other experimentation shows that the heating in the Indonesian region has some impact on σ_{BI} in this Pacific storm-track region. Again, Fig. 9d mimics the

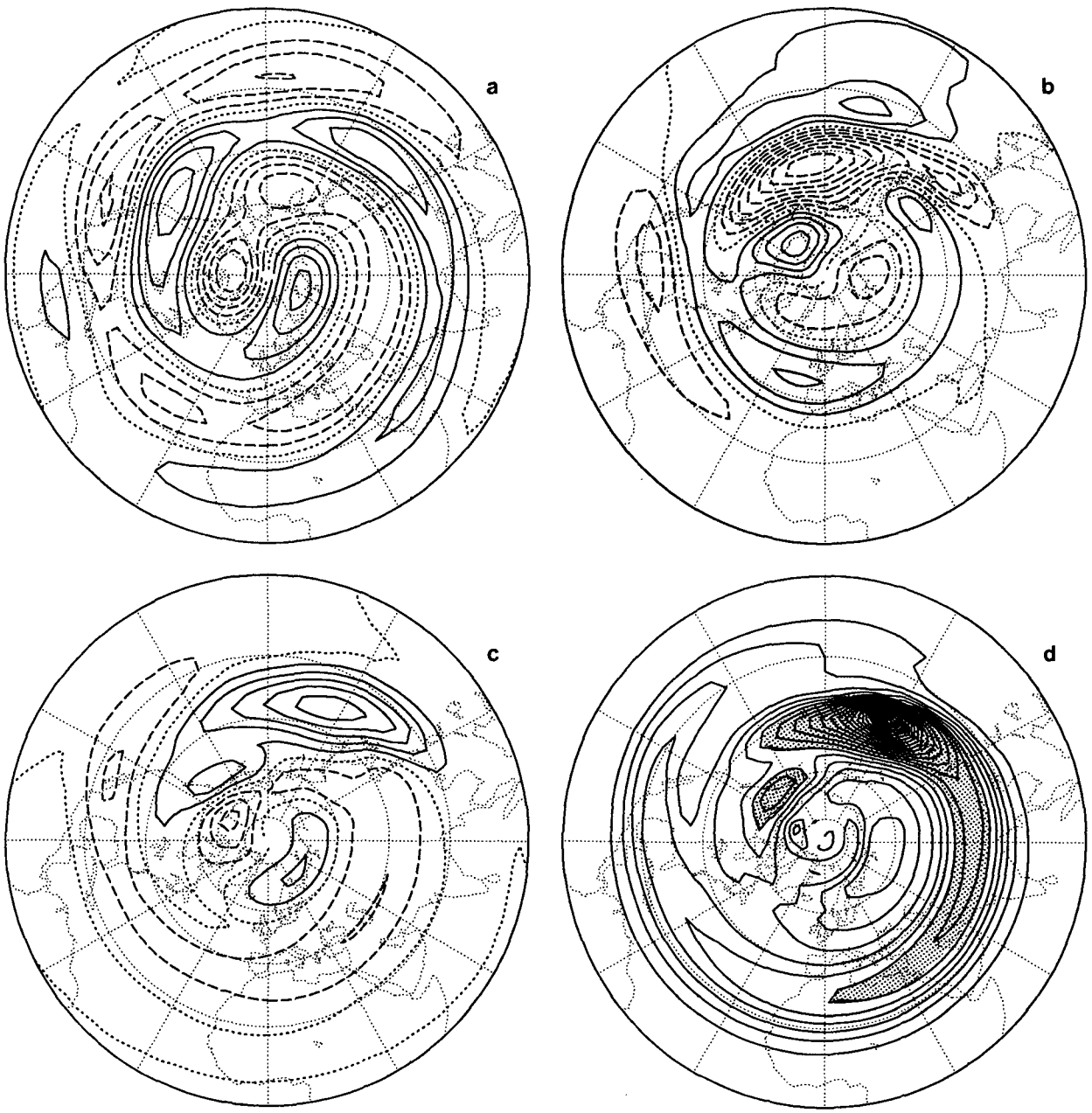

FIG. 9. The steady state, linear response to North Pacific storm-track forcing by synoptic time scale transients and mean diabatic heating. Shown are (a) the upper level streamfunction, (b) the lower level streamfunction, (c) the lower level temperature, and (d) the baroclinicity parameter σ_{BI}. The conventions are as in Fig. 4.

observed tendency to confine the storm-track longitudinally with low values of σ_{BI} downstream of the maximum.

5. Concluding remarks

The results of the linear, stationary wave model strongly suggest that the crucial ingredient in the existence of mean conditions suitable for the existence of the two Northern Hemisphere storm-tracks is the mean diabatic heating in the region of the storm-tracks, off the east coast of the continents. Given the mean baroclinicity it is entirely consistent that the development of weather systems is biased towards the two regions. The large-scale latent heat release indeed acts to invigorate individual weather systems as it occurs in the warm air. The low-level sensible heating in the cold air could act to intensify surface low-pressure centers but its overall effect, as measured by $\overline{Q'T'}$, will be to act to decrease the energy in the systems. To initiate the growth process in the storm-track regions, an initial

disturbance is required. The debris from previous weather systems may be sufficient, though it is possible that the interaction of the atmosphere with the upstream mountain chains could play an important role in providing suitable disturbances.

It is probable that the rather crude high-pass filter used here underestimates the magnitude of the transient eddies in the synoptic time scale. It is also possible that the low-level diabatic heating input into the model is rather strong. However, the conclusions from the solutions discussed here are quite robust to such errors.

In this paper we have examined the Northern Hemisphere storm-tracks. The Southern Hemisphere does not provide the necessary middle latitude continent–ocean contrast, and its extended but less definite storm-track could be rather different in its maintenance (cf. James and Anderson 1983).

As was done in the Introduction, it can be argued that the diabatic heating maxima in the storm-track regions are caused by horizontal and vertical displacements associated with individual storms. Thus, in some senses the North Atlantic and Pacific storm-tracks are self-maintaining. However, to base this argument on a firmer foundation we need to be able to state what the atmosphere, and in particular σ_{BI}, would look like in the absence of the eddies. Such a steady solution has not been obtained and indeed would probably be extremely sensitive to the representation of small scale mixing processes. One argument is that one should compare the observed state with that given by assuming moist, convectively neutral profiles from the sea surface temperature (K. Emanuel, personal communication). Such a state would have midlatitude oceanic values of σ_{BI} larger than those shown in Fig. 2 for the observed state, particularly in the Gulf Stream region. In this context it would be said that the storm-track is in balance with a weakened baroclinicity.

There is no doubt that the warm oceans off the east coasts of the cold North American and Asian continents provide the conditions in which winter storm-tracks are inevitable. This raises another way in which storm-tracks can be viewed as contributing to their self-maintenance. The low-level mean flows induced by all the eddy effects (Figs. 7b and 9b), as with the observed flow, have wind-stress curls that are in the sense of driving the warm Gulf Stream and Kuroshio. Thus, the storm-tracks act to drive the warm western boundary currents, which in turn are crucial to the existence of the storm-tracks.

Acknowledgments. We wish to thank I. Held and the two reviewers for helpful comments on an earlier version of this paper.

REFERENCES

Blackmon, M. L., 1976: A climatological spectral study of the 500 mb geopotential height of the Northern Hemisphere. *J. Atmos. Sci.*, **33**, 1607–1623.

Charney, J. G., 1947: The dynamics of long waves in a baroclinic current. *J. Meteor.*, **4**, 125–162.

Emanuel, K. A., M. Fantini and A. J. Thorpe, 1987: Baroclinic instability in an environment of small slantwise moist convection. Part I: Two-dimensional models. *J. Atmos. Sci.*, **44**, 1559–1573.

Frederiksen, J. S., 1983: Disturbances and eddy fluxes in Northern Hemisphere flows: Instability of three dimensional January and July flows. *J. Atmos. Sci.*, **40**, 836–855.

Held, I. M., 1987: The vertical scale of an unstable baroclinic wave and its importance for eddy heat flux parameterisations. *J. Atmos. Sci.*, **35**, 572–576.

Hoskins, B. J., 1983: Modelling of the transient eddies and their feed-back on the mean flow. *Large-scale Dynamical Processes in the Atmosphere*, B. J. Hoskins, R. P. Pearce, Eds., Academic Press, 169–199.

——, and A. J. Simmons, 1975: A multi-layer spectral model and the semi-implicit method. *Quart. J. Roy. Meteor. Soc.*, **101**, 637–655.

——, I. N. James and G. H. White, 1983: The shape, propagation and mean-flow interaction of large-scale weather systems. *J. Atmos. Sci.*, **40**, 1595–1611.

James, I. N., 1987: Suppression of baroclinic instability in horizontally sheared flows. *J. Atmos. Sci.*, **44**, 3710–3720.

——, and D. L. T. Anderson, 1983: The seasonal mean flow and distribution of large-scale weather systems in the southern hemisphere: The effects of moisture transports. *Quart. J. Roy. Meteor. Soc.*, **110**, 943–966.

Lau, N.-C., and J. M. Wallace, 1979: On the distribution of horizontal transport by transient eddies in the Northern Hemisphere wintertime circulation. *J. Atmos. Sci.*, **36**, 1844–1861.

——, G. H. White and R. L. Jenne, 1981: Circulation statistics for the extratropical Northern Hemisphere based on NMC analyses. NCAR Tech. Note TN-171 + STR, 138 pp.

Lindzen, R. S., and B. Farrell, 1980: A simple approximate result for the maximum growth rate of baroclinic instabilities. *J. Atmos. Sci.*, **37**, 1648–1654.

Lorenz, E. N., 1979: Forced and free variations of weather and climate. *J. Atmos. Sci.*, **36**, 1367–1376.

Sardeshmukh, P. D., and B. J. Hoskins, 1984: Spatial smoothing on the sphere. *Mon. Wea. Rev.*, **112**, 2524–2529.

Simmons, A. J., and B. J. Hoskins, 1979: The downstream and upstream development of unstable baroclinic waves. *J. Atmos. Sci.*, **36**, 1239–1254.

——, and ——, 1980: Barotropic influences on the growth and decay of nonlinear baroclinic waves. *J. Atmos. Sci.*, **37**, 1679–1684.

Stephens, G. L., and P. J. Webster, 1979: Sensitivity of radiative forcing to variable cloud and moisture. *J. Atmos. Sci.*, **36**, 1542–1556.

Sutcliffe, R. C., 1951: Mean upper contour patterns of the Northern Hemisphere—the thermal-synoptic view pattern. *Quart. J. Roy. Meteor. Soc.*, **77**, 435–440.

Valdes, P. J., and B. J. Hoskins, 1989: Linear stationary wave simulations of the time mean climatological flow. *J. Atmos. Sci.*, **46**, 2509–2527.

Wallace, J. M., G.-H. Lim and M. L. Blackmon, 1988: Relationship between cyclone tracks, anticyclone tracks and baroclinic waveguides. *J. Atmos. Sci.*, **45**, 439–462.